JAAS

PAPER

View Article Online
View Journal | View Issue

In situ U–Pb dating of bastnaesite by LA-ICP-MS

Cite this: *J. Anal. At. Spectrom.*, 2014, **29**, 1017

Yue-Heng Yang,*[a] Fu-Yuan Wu,[a] Yang Li,[ab] Jin-Hui Yang,[a] Lie-Wen Xie,[a] Yan Liu,[c] Yan-Bin Zhang[a] and Chao Huang[a]

Bastnaesite, a common accessory mineral in REE ore deposits, is ideal for U–Pb isotopic dating because of its relatively high U and Th contents. We report an analytical procedure for U–Pb dating of this mineral using a 193 nm ArF excimer laser ablation system coupled to an Agilent 7500a (LA-ICP-MS). Laser induced elemental fractionation and instrumental mass discrimination were externally corrected using an in house bastnaesite standard (K-9). The fluence, spot size and repetition rate of laser were evaluated to assess their effects on age determination in detail. The matrix effect on zircon and bastnaesite was also investigated and compared in detail during laser sampling. The results indicate that a matrix-matched standard reference material is essential. In order to validate and demonstrate the effectiveness and robustness of our developed protocol, we dated several bastnaesite samples from the Himalayan Mianning-Dechang REE belt, South-West China. The U–Pb ages of ~31 to 34 Ma obtained for bastnaesites from Maoniuping, Diaoloushan, Zhengjialiangzi and Lizhuang are in good agreement within error, but differ from the wide range of age (10–40 Ma) obtained using K–Ar and Ar–Ar methods for biotite and muscovite and using U–Pb dating for zircon. These dating applications demonstrate the reliability and feasibility of our established method. In summary, the LA-ICP-MS dating of bastnaesite can be a complementary dating method to the more established TIMS and SIMS techniques with advantages of rapidity, moderate spatial resolution and relatively low cost.

Received 3rd January 2014
Accepted 10th March 2014

DOI: 10.1039/c4ja00001c

www.rsc.org/jaas

1. Introduction

The ability to accurately determine the time of mineralization is crucial for understanding the genesis of endogenous ore deposits and formation processes.[1] According to the present knowledge, numerous radiometric dating methods have been applied to date mineralization, including K (Ar)–Ar, Rb–Sr, Sm–Nd, Lu–Hf, Re–Os and U–Pb techniques. Among these techniques, the U–Pb method has been considered as the most powerful tool for obtaining precise and accurate age of mineralization. However, for most ore deposits, the U–Pb method is not applicable due to the lack of suitable minerals. This problem is also encountered in dating rare earth elements (REE) deposits, which are generally related to the occurrences of alkaline and carbonatite rocks.[1–3]

Bastnaesite (Bastnäsite, $(Ce)CO_3F$), a carbonate-fluoride mineral, is a common accessory mineral in REE ore deposits. It was first described by the Swedish chemist Wilhelm Hisinger in 1838 and named after the Bastnäs mine near Riddarhyttan, Västmanland, Sweden. This mineral can occur as a very high quality specimen (Zagi Mountains, Pakistan), but mostly occurs in alkali granite, syenite and associated pegmatite, and carbonatite. The mineral has a variable composition of La, Ce, Nd, Y and Ba and forms a group mineral of bastnaesite, parasite, cordylite, Huangheite, cebaite and Zhonghuacerite. Nonetheless, bastnaesite is one of the most important REE carriers as monazite (Mountain Pass in USA, and Bayan Obo in China). In contrast to monazite, however, bastnaesite is less investigated for U–(Th)–Pb and other isotopic systems, despite its fairly wide occurrence or distribution in carbonatites, alkaline rocks, and associated REE deposits.[2–5]

To the best of our knowledge, bastnaesite has been dated using the La–Ba method by traditional isotopic dilution thermal ionization mass spectrometry (ID-TIMS).[6] Using this method, an isochron age of 586.8 ± 3.7 Ma was obtained for the bastnaesite from the Gakara deposit in Burundi. The pioneering work on the Bayan Obo deposit by Wang *et al.*[2] indicated that bastnaesite there contains a much lower amount of U (mostly less than 0.5 ppm), which makes it impossible to determine its U–Pb age, although a Th–Pb age of 555–475 Ma was obtained. Considering that the associated monazite contains an extremely low amount of U as well, it is unknown whether bastnaesite in other areas contain a similar U concentration. Recently, however, Sal'nikova *et al.*[4] conducted a U–Pb isotopic analysis for the bastnaesite from the Karasug carbonatite in central Mongolia and obtained a concordant age of 118 ± 1 Ma. Therefore, it was demonstrated that bastnaesite could be an

[a]*State Key Laboratory of Lithospheric Evolution, Institute of Geology and Geophysics, Chinese Academy of Sciences, P. B. 9825, Beijing, 100029, P.R. China. E-mail: yangyueheng@mail.iggcas.ac.cn; Fax: +86-010-62010846; Tel: +86-010-82998599*
[b]*School of Earth Sciences, Graduate University of Chinese Academy of Sciences, Beijing, 100039, P.R. China*
[c]*Institute of Geology, Chinese Academy of Geological Sciences, Beijing, 100037, P.R. China*

important mineral for constraining the age of REE mineralization. It is also interesting to note that the obtained $^{206}Pb/^{204}Pb$ ratios for the two analyses were 488 (U of 222 ppm) and 1440 (U of 653 ppm), which correspond to 3.8% and 1.3%, respectively, of f_{206} ratios. Considering that the studied samples were formed in the Mesozoic, most bastnaesite, especially those formed in the Precambrian, might have low to negligible common lead, as do usually dated minerals of zircon, baddeleyite, monazite and xenotime. However, most REE deposits have a complicated history due to intensive fluid activities. For example, the formation age of the Bayan Obo, the most important REE deposit in the world, is still in debate due to later alteration.[2,3] In this case, an *in situ* U–Pb analytical technique is desired to decipher the complex history of REE mineralization.

In addition, the crystal structure of bastnaesite can accommodate high concentrations of light rare earth elements (LREE), with a Nd content of ~10 wt%, which makes it an ideal candidate for *in situ* Nd isotopic analyses.[5] This kind of data would definitively provide important information on the origin and genesis of the ore deposits.[1] Therefore, in this study, we developed an *in situ* protocol of U–Pb dating bastnaesite by LA-ICP-MS and explored its application as a dating method. The fluence, spot size and repetition rate of the laser were evaluated to check the age of bastnaesite in detail. The matrix effect on zircon and bastnaeiste was also investigated. The reliability and validity of the proposed methodology was tested using samples of bastnaesite collected in the Himalayan Mianning-Dechang REE belt, South-West China. These samples were previously dated by conventional Rb–Sr, Ar–Ar and U–Pb dating methods. Our results indicate that bastnaesite can contain a significant amount of common Pb and therefore indicate that a common Pb correction is necessary in order to obtain a correct U–Pb age, which differs from the previous observation.[1]

2. Experimental

All bastnaesite samples investigated in this work were analyzed for major, trace element concentrations and U–Th–Pb ages by *in situ* LA-ICP-MS techniques. All analyses were conducted at the State Key Laboratory of Lithospheric Evolution of the Institute of Geology and Geophysics, Chinese Academy of Sciences, Beijing, China.

2.1. Sample preparation

All bastnaesite grains were mounted in epoxy in 2.5 cm diameter circular grain mounts and polished until the bastnaesite grains were just revealed. Transmitted, reflected and back-scattered electron microscopic images were used to examine the internal structure, such as inclusions, crack and growth zones which provided a base map for selection of ablation spots. The grain mount was cleaned and left in 2% HNO_3 for several minutes prior to laser ablation analysis.[7]

2.2. Bastnaesite reference material

Well-characterized, matrix-matched reference material is crucial for an *in situ* analytical technique. Unlike other widely distributed and well-characterized mineral standards such as zircon (*e.g.*, 91 500, *etc.*), monazite (*e.g.*, 44 069, *etc.*), apatite (*e.g.*, Durango, *etc.*) and titanite (*e.g.*, BLR-1 *etc.*), so far, there is no reported reference bastnaesite material for *in situ* laser ablation. The primary bastnaesite *in house* reference standard analyzed in this study was K-9, which yielded a TIMS concordian age of 118 ± 1 Ma (MSWD = 0.05, probability = 0.82). This standard was collected from the supergene-altered, hematite-bearing siderite carbonatite with baritocelestine. Moreover, its ID-TIMS U–Pb age is in excellent agreement with the Sm–Nd ages obtained for bastnaesite and fluorite from the carbonatite and is also consistent with the age of 118 ± 9 Ma obtained by the Rb–Sr method for mica from carbonatites. A detailed description of sample location can be found in SalNikova *et al.*[4]

2.3. Instrumentation

Experiments were carried out using an Agilent 7500a ICP-MS (Agilent Technologies, Japan) in combination with an excimer 193 nm laser ablation system (Geolas 2005, Lambda Physik, Gottingen, Germany). The laser spot size was adjusted to 5, 10, 16, 24, 32, 44, 60, 90, 120 and 160 μm, and the frequency can be adjusted from 1 to 20 Hz.[8]

2.4. Mass spectrometry

The analytical procedure for bastnaesite U–Th–Pb dating and trace element compositions (including REE) was similar to that for the zircon, monazite and apatite dating by LA-ICP-MS. A summary of the LA-ICP-MS specifications and typical operating conditions used in this study is presented in Table 1. Helium was used as the carrier gas through the ablation cell and was merged with argon (make-up gas) downstream the ablation cell.[9] Prior to analysis, the Pulse/Analogy (P/A) factor of the detector was calibrated using standard tuning solution. The carrier and make-up gas flows were optimized to obtain maximum signal intensity for $^{238}U^{+}$, while keeping the

Table 1 Typical operating conditions for *in situ* U–Pb dating of bastnaesite

Agilent 7500a ICP-MS	
RF power	1350 W
Cooling gas	15 L min^{-1}
Auxiliary gas	1.0 L min^{-1}
Sample gas	0.85 L min^{-1}
Ion optic settings	Typical
Detector mode	Dual
Sensitivity	200 Mcps/ppm on ^{89}Y signal *via* 100 mL min^{-1} PFA nebulizer
Integration time	6 ms for Rb, Sr, Ba, Nb, Ta, Zr, Hf and REE, 15 ms for ^{204}Pb, ^{206}Pb & ^{208}Pb, 30 ms for ^{207}Pb, 10 ms for ^{232}Th & ^{238}U
GeoLas 2005 laser ablation system	
Wavelength	193 nm, excitation laser
Pulse length	15 ns
Energy density	4, 6, 8, 10 J cm^{-2}
Spot size	16, 32, 44, 60 μm
Repetition rate	4, 6, 8, 10 Hz
Carrier gas	Helium (~0.85 L min^{-1})

ThO^+/Th^+ ratio below 0.5%. All LA-ICP-MS measurements were carried out using time resolved analysis in the fast, peak jumping mode. Each spot analysis consisted of an approximate 20 s background acquisition and a 65 s sample data acquisition. The dwell time for each isotope was set at 6 ms for Rb, Sr, Ba, Nb, Ta, Zr, Hf and REE; 10 ms for ^{232}Th and ^{238}U; 15 ms for ^{204}Pb, ^{206}Pb, and ^{208}Pb; and 30 ms for ^{207}Pb. A matrix-matched external bastnaesite standard (K-9) was used to correct for U–Th–Pb fractionation and instrumental mass discrimination. Two K-9 analyses were measured after every five unknown bastnaesite spots. In this work, the cratering model rather than rastering ablated model was adopted, and the total ablated time was about 60 seconds for a single standard or sample measurement.

2.5. Data reduction

Signals of ^{204}Pb, ^{206}Pb, ^{207}Pb, ^{208}Pb, ^{232}Th and ^{238}U were acquired for U–Pb dating, whereas the ^{235}U signal was calculated from ^{238}U on the basis of the ratio $^{238}U/^{235}U = 137.88$. All the measured $^{207}Pb/^{206}Pb$, $^{207}Pb/^{235}U$ and $^{206}Pb/^{238}U$ isotopic ratios of the K-9 standard during the process of sample analyses were regressed and corrected using the reference values. The concordia age of 118 Ma was used as the reference value.[4] Standard deviations of the calibrated isotope ratios include those from the sample, external standard, and deviations from the reference values of external standard. The uncertainty was set at 2%. The U–Pb concordia ages and weighted mean ages were calculated using the ISOPLOT/EX 3.23 software package.[10] Trace concentrations were calibrated against the NIST SRM 610 as an external reference material using ^{140}Ce as an internal standard using the Glitter software.[11] Ce was used as an internal standard for calibration purposes.

Accurate correction for laser induced elemental fractionation and instrumental drift is an important consideration in U–Pb dating of accessory minerals in LA-ICP-MS measurements. In this study, we used the well-characterized, matrix-matched in house K-9 standard protocol to correct for U–Pb elemental fractionation and variations in sensitivity during an analytical session. The procedure is similar to the one used for zircon dating by LA-ICP-MS with GJ-1 or 91 500 standard.[11,12] Another significant difficulty of U–Pb dating of bastnaesite is the present high common Pb content, which is incorporated from the parental magma in the early phase of mineral crystallization.[13,14] As recently noted by Chew *et al.*,[13] common Pb correction is typically undertaken using either concordia or isochron plots on a suite of co-genetic grains or alternatively on individual analyses using an appropriate choice of initial Pb isotopic composition. In this study, the ^{207}Pb correction method was applied for common Pb correction using the

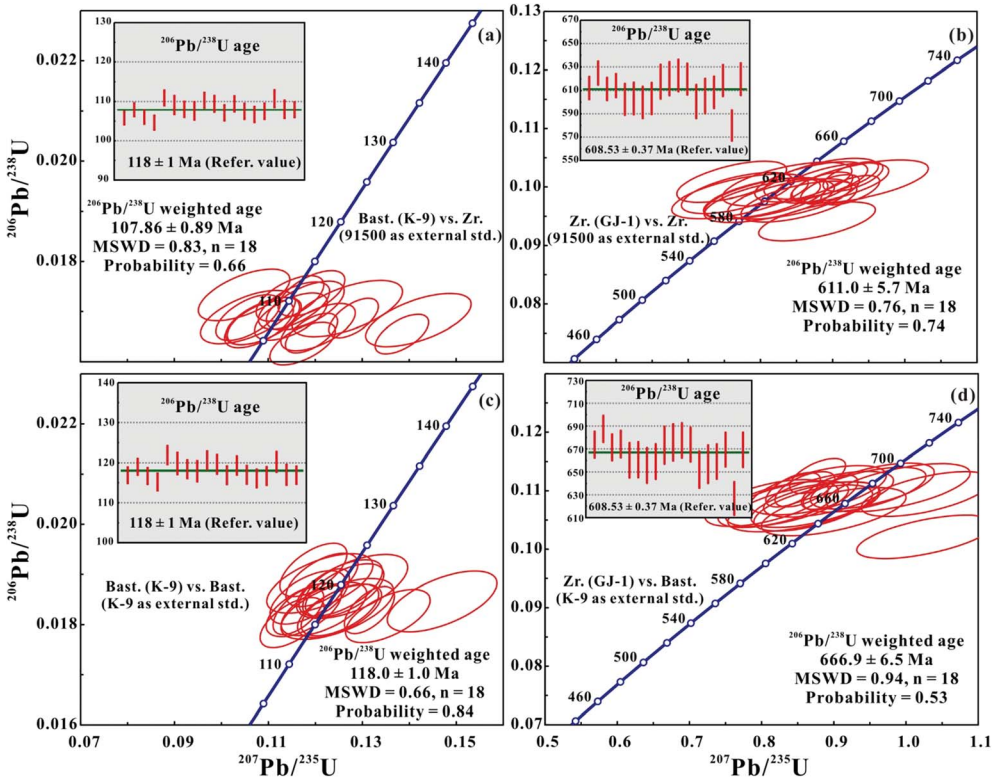

Fig. 1 Matrix effect on bastnaesite and zircon is investigated in detail during laser sampling U–Pb dating. The results show that there is significant matrix effect on these minerals. Panels a and b show the weighted average $^{206}Pb/^{238}U$ ages of bastnaesite (K-9) and zircon (GJ-1) samples using the zircon standard (91500) for external calibration, whereas panels c and d show that of bastnaesite (K-9) and zircon (GJ-1) samples using bastnaesite (K-9) as the external calibration standard during the same analytical session, indicating that a suitable matrix-matched standard is crucial for *in situ* U–Pb dating of bastnaesite using LA-ICP-MS. The MSWD shows the mean square of weighted deviates.

two-stage model of Stacey and Kramers[15] (refer also to Williams[16]), and the $^{206}Pb/^{238}U$ weighted ages were calculated using Isoplot 3.23. Moreover, the intercepts of regression lines through the raw data on a Tera–Wasserburg plot provide an estimate of the $^{207}Pb/^{206}Pb$ for the common Pb component (upper intercept) and the inferred crystallization age (lower intercept).[14,17,18]

3. Results and discussion

3.1. Matrix effect

The lack of well-characterized matrix-matched reference materials to correct for elemental fractionation is a significant obstacle for *in situ* U–Pb dating of accessory minerals by LA-ICP-MS or SIMS techniques. Therefore, we first evaluated the matrix effect on *in situ* U–Pb age analysis of bastnaesite (K-9) and zircon (GJ-1) reference materials using zircon standard 91 500 as an external calibration standard during the same analytical session. When the 91 500 zircon was used as an external calibration standard, the obtained weighted $^{206}Pb/^{238}U$ age for the K-9 standard was 107.86 ± 0.89 Ma (MSWD = 0.83, n = 18, Fig. 1a), which is 10% younger than the published reference value of 118 ± 1 Ma.[4] However, the weighted $^{206}Pb/^{238}U$ age of 611.0 ± 5.7 Ma (MSWD = 0.76, n = 18, Fig. 1b) for GJ-1 agrees well with the published recommended value obtained using ID-TIMS (608.53 ± 0.37 Ma).[19] Similarly, when bastnaesite K-9 was used as an external calibration standard, the weighted $^{206}Pb/^{238}U$ age of K-9 as an unknown sample was 118.0 ± 1.0 Ma (MSWD = 0.66, n = 18), which is in excellent agreement with the classic ID-TIMS data.[4] However, the weighted $^{206}Pb/^{238}U$ age (666.9 ± 6.5 Ma, MSWD = 0.94, n = 18) of GJ-1 is 10% older than the reference value.[19] These results means that there are significant matrix effects between bastnaesite and zircon during laser ablation, indicating that a suitable matrix-matched standard is essential and crucial for *in situ* U–Pb dating of bastnaesite using LA-ICP-MS. Although the exact reason for the significant matrix effect is still unknown, a similar situation was previously observed and reported for titanite, allanite, xenotime, monazite and zircon during *in situ* U–Pb dating by a LA-ICP-MS technique.[20–23]

3.2. Laser spot size, repetition rate and fluence

Ablation experiments on the bastnaesite (K-9) grain were carried out using a spot ablation routine at repetition rates of 4, 6, 8 and 10 Hz and sample fluences of 4, 6, 8 and 10 J cm^2. Spot sizes of 16, 32, 44 and 60 μm were used to obtain enough intensity for the less abundant isotopes and to avoid potential zonation. As shown in Fig. 2a–d and Table 2, at a constant repetition rate of 8 Hz and 44 μm crater size, with increasing fluences of 4, 6, 8 and 10 J cm^2, the obtained weighted $^{206}Pb/^{238}U$ ages of K-9 for every ten analyses were 125.5 ± 2.0 Ma (MSWD = 1.07, 4 J cm^{-2}), 116.9 ± 1.6 Ma (MSWD = 0.73, 6 J cm^{-2}), 117.3 ± 1.5 Ma (MSWD = 0.50, 8 J cm^{-2}) and 117.4 ± 1.5 Ma (MSWD = 0.33, 10 J cm^{-2}), respectively. Similarly, as shown in Fig. 2e–g, at a constant repetition rate of 8 Hz and fluence of 8 J cm^2, with increasing crater size of 16, 32 and 60 μm, the above ages were

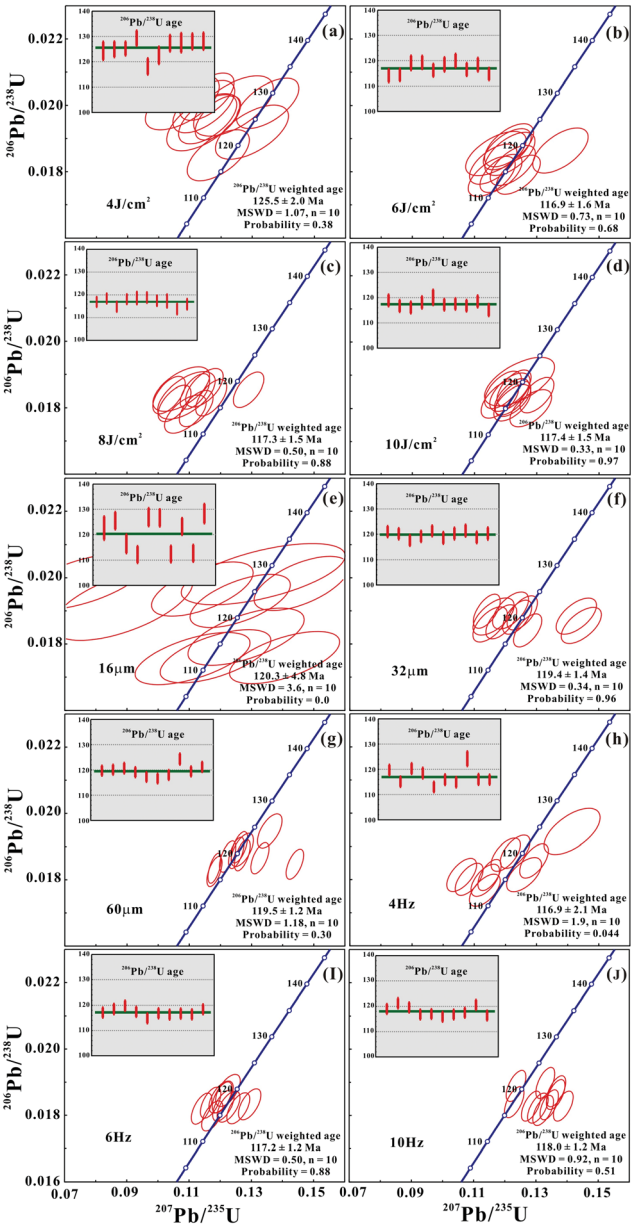

Fig. 2 Weighted average $^{206}Pb/^{238}U$ ages of K-9 bastnaesite calculated during the same analytical session using 16-, 32-, and 60 μm spot sizes at repetition rates of 4, 6, and 10 Hz and sample fluence of 4, 6 and 10 J cm^{-2} under the external standard fixed laser parameter using a 44 μm spot size at a repetition rate of 8 Hz and a sample fluence of 8 J cm^2. The MSWD shows the mean square of weighted deviates.

120.3 ± 4.8 Ma (MSWD = 3.6, 16 μm), 119.4 ± 1.4 Ma (MSWD = 0.34, 32 μm) and 119.5 ± 1.2 Ma (MSWD = 1.18, 60 μm), respectively. Additionally, as shown in Fig. 2h–j, at a constant fluence of 8 J cm^{-2} and 44 μm crater size, with increasing repetition rate from 4, 6 and 10 Hz, our obtained weighted $^{206}Pb/^{238}U$ ages of ten analyses for each were 116.9 ± 2.1 Ma (MSWD = 1.9, 4 Hz), 117.1 ± 1.2 Ma (MSWD = 0.50, 6 Hz) and 118.0 ± 1.2 Ma (MSWD = 0.92, 10 Hz), respectively. The above experiments indicate that there is no significant age variation with variable spot size, repetition rate and fluence intensity. As shown in Fig. 2 and Table 2, the spot size has a more significant

Table 2 Age comparison with different laser experimental parameters

1. Fluence (changing) (fixed 44 μm & 8 Hz)	4 J cm^{-2}	6 J cm^{-2}	8 J cm^{-2}	10 J cm^{-2}
^{206}Pb/^{238}U weighted age (Ma)	125.5 ± 2.0	116.9 ± 1.6	117.3 ± 1.5	117.4 ± 1.5
[MSWD]	[1.07]	[0.73]	[0.50]	[0.33]
[Probability]	[0.38]	[0.68]	[0.88]	[0.97]
2. Spot size (μm) (changing) (fixed 8 J cm^{-2} & 8 Hz)	16 μm	32 μm		60 μm
^{206}Pb/^{238}U weighted age (Ma)	120.3 ± 4.8	119.4 ± 1.4		119.5 ± 1.2
[MSWD]	[3.6]	[0.34]		[1.18]
[Probability]	[0]	[0.96]		[0.30]
3. Repetition rate (changing) (fixed 44 μm & 8 J cm^{-2})	4 Hz	6 Hz		10 Hz
^{206}Pb/^{238}U weighted age (Ma)	116.9 ± 2.1	117.2 ± 1.2		118.0 ± 1.2
[MSWD]	[1.9]	[0.50]		[0.92]
[Probability]	[0.044]	[0.88]		[0.51]

effect on the age error than repetition rate and fluence because of its less ablated material and less intensity signal (*e.g.*, 16 μm). Therefore, a spot size of 44 μm was applied with a repetition rate of 8 Hz, corresponding to an energy density of ~10 J cm^{-2}, in the following sample analyses.

4. Application

In order to demonstrate the effectiveness and robustness of our developed protocol, we dated numerous bastnaesite samples and compared the results with available published data. The bastnaesite grains were prepared following the procedure described in the sample preparation subsection. The chemical compositions of theses samples for REE contents are listed in the Appendix, and the REE patterns are shown in Fig. 3.

As is well known, the Himalayan Mianning-Dechang (MD) REE belt, western Sichuan, SW China, is approximately 270 km long and 15 km wide and contains total reserves of more than 3 Mt of LREE, including one giant (Maoniuping), one large (Dalucao) and a number of small-medium REE deposits (Moluozhai and Lizhuang).[24–27] REE mineralization is associated with Himalayan carbonatite–alkaline complexes, which consist of carbonatitic sills or dykes and associated alkaline syenite stocks. A few available dating data define a Himalayan metallogenic epoch (10–40 Ma) by a K–Ar or Ar–Ar method for biotite and muscovite or U–Pb dating of zircon by SHRIMP.[25–27]

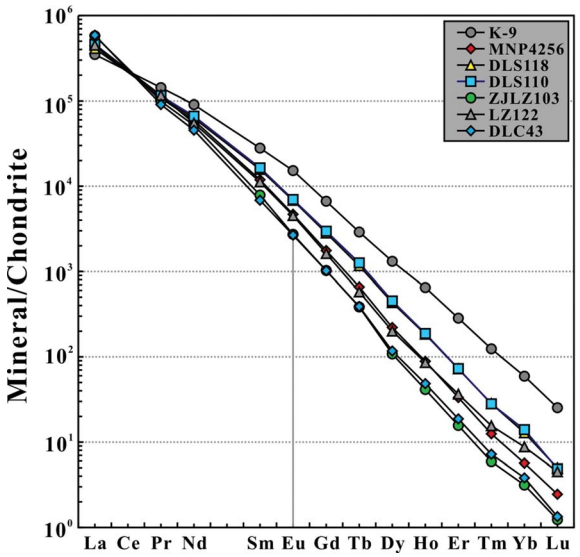

Fig. 3 Chondrite-normalized REE distribution pattern of bastnaesite.

The Maoniuping (MNP) is a world-class REE deposit, following only the Bayan Obo REE-Nb-Fe (China) and Mountain Pass (USA) REE deposits in terms of size. Previously, K–Ar dating of hydrothermal minerals (biotite and magnesio-arfvedonite) yielded an age ranging from 27.8 ± 0.5 Ma to 40.3 ± 0.7 Ma,[28] indicating a relatively wide REE mineralization age for this deposit. The analysed sample of MNP4256 contained ~11 ppm of U and ~2467 ppm of Th, with a Th/U ratio of ~243. Twelve analyses yielded a lower intercept age of 31.1 ± 3.9 Ma, which is identical to the ^{207}Pb corrected age of 30.7 ± 3.0 Ma (Fig. 4a). Therefore, we consider that this deposit was formed ~31 Ma.

Muluozhai is composed of two small deposits of Diaoloushan (DLS) and Zhengjialiangzi (ZJLZ). The obtained K–Ar ages from potassium feldspar and phlogpite were 31.2 and 35.5 Ma, respectively. The analysed sample of DLS contained ~16 (DLS108) and ~12 (DLS110) ppm of U and ~2220 (DLS108) and ~1603 (DLS110) ppm of Th, with Th/U ratios of ~144 (DLS108) and ~136 (DLS110), respectively. The obtained intercept ages were 32.2 ± 2.6 Ma (DLS108) and 34.9 ± 3.1 Ma (DLS110), with ^{207}Pb corrected ages of 31.8 ± 2.1 Ma (DLS108) and 33.0 ± 2.6 Ma (DLS110) (Fig. 4b and c). For the Zhengjialiangzi deposit, the analysed sample of ZJLZ103 contained ~7.8 ppm of U and ~1826 ppm of Th, with a Th/U ratio of ~272. Nineteen analyses for the sample yielded an intercept and ^{207}Pb corrected ages of 33.3 ± 3.3 and 33.3 ± 2.6 Ma, which are identical to those obtained from the Maoniuping deposit.

Another deposit in the area is Lizhuang (LZ), which gives a K–Ar age ranging between 27.1 and 30.6 Ma. The analysed sample of LZ122 contained ~27 ppm of U and ~4555 ppm of Th, with a Th/U ratio of ~167. During this study, sample LZ122 was collected for U–Pb analysis, and the obtained intercept and ^{207}Pb corrected ages were 32.9 ± 3.7 and 33.0 ± 2.1 Ma, respectively (Fig. 4e), consistent with those from the Maoniuping and Muluozhai deposits.

Dalucao (DLC) is the second largest deposit in the MD REE belt. The obtained K–Ar ages from biotite and muscovite ranged from 9.8–14.5 Ma,[29] which is slightly younger than the Rb–Sr isochron age of 15.3 ± 0.5 Ma for REE ores. U–Pb dating of

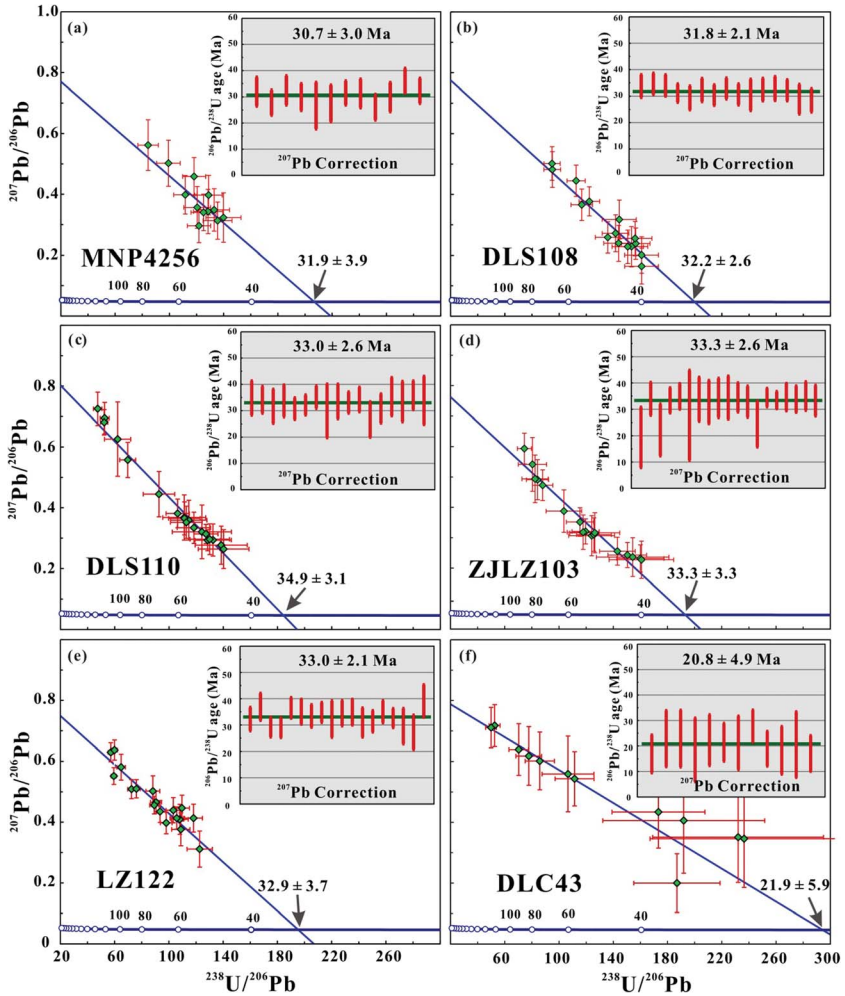

Fig. 4 Tera–Wasserburg plots for *in situ* U–Pb data and ^{207}Pb common lead correction for five different localities of bastnaesite from the Mianning-Dechang belt REE deposits (Sichuan, SW China). Error bars show 1 s errors. These results indicate that the narrow mineralization age of the Mianning-Dechang REE belt is consistent with biotite K–Ar and Ar–Ar ages within error.

zircons from carbonatite and syenite yielded ages of 12.99 ± 0.94 and 14.53 ± 0.31 Ma, respectively.[26] Our analysed sample of DLC43 contained ~3.0 ppm of U and ~475 ppm of Th, with a Th/U ratio of ~158. Twelve analyses on this sample yielded a lower intercept age of 21.9 ± 5.9 Ma, with a ^{207}Pb corrected age of 20.8 ± 4.9 Ma (Fig. 4f), about 10 Ma younger than those from the other deposits presented above. However, it is noted that the ages obtained for this sample show larger errors than the other samples studied due to its lower U concentration.

The age data presented above indicated that all of the deposits in the area were synchronously formed at ~31 to 34 Ma, consistence with the K–Ar or Ar–Ar ages for most deposits, except Dalucao. For the latter, our U–Pb age is significantly older than the reported K–Ar, Rb–Sr and U–Pb ages. Although this discrepancy needs more analyses to be verified, the consistency of ages among other deposits suggests that our data are reliable. This practical dating example demonstrated the applicability and promising prospect of using our developed methodology for dating commonly bastnaesite-bearing carbonatite, alkaline rocks and related REE deposits in the near future.[1] Moreover, it is noted from the data that our samples contained a significant amount of common lead, although the exact amounts are not available from laser ablation analyses.

5. Conclusions

In this contribution, we demonstrated the possibility of using bastnaesite as a dating mineral for U–Pb geochronology using LA-ICP-MS. The relatively easy sample preparation and operating system combined with the short running time make it an ideal mineral for dating bastnaesite-bearing rocks. Laser induced elemental fractionation and instrumental mass discrimination were externally corrected using the reference material K-9. The laser fluence, spot size and repetition rate were evaluated to assess the quality of the obtained age in detail. The matrix effect on zircon and bastnaesite was investigated and compared in detail during laser sampling. Our results indicate that the matrix effects of bastnaesite and zircon maybe significant. In order to validate and demonstrate the efficacy and strength of our developed protocol, we tested the *in situ*

U–Pb dating application on several bastnaesite samples collected in SW China, which show the reliability of our established method. The minerals of the bastnaesite group have a fairly wide distribution and a relatively high U and Th Pb contents, making it an ideal mineral for U–Pb isotopic dating. LA-ICP-MS can be considered a promising geochronological tool suitable for U–Pb dating of carbonatites, alkaline rocks, and related REE deposits.

Acknowledgements

This study was financially supported by the Natural Science Foundation of China (NSFC Grants 41273021, 41221002 and 41130313). We are greatly indebted to Dr E. B. Sal'Nikova for kindly providing the K-9 bastnaeiste standard. We are particularly thankful to Dr Yamirka Rojas-Agramonte for correcting the English. We also thank Laura Petley for her patience while handling our manuscript and also are grateful for the critical and insightful comments from two anonymous referees who improved the quality of the manuscript.

References

1 F. Robert, *Nature*, 1990, **364**, 792–793.
2 J. W. Wang, M. Tatsumoto, X. B. Li, W. R. Premo and E. C. T. Chao, *Geochim. Cosmochim. Acta*, 1994, **58**, 3155–3169.
3 M. X. Ling, Y. L. Liu, I. S. Williams, F. Z. Teng, X. Y. Yang, X. Ding, G. J. Wei, L. H. Xie, W. F. Deng and W. D. Sun, *Sci. Rep.*, 2013, **3**, 1776, DOI: 10.1038/srep01776.
4 E. B. Sal'nikova, S. Z. Yakovleva, A. V. Nikiforov, A. B. Kotov, V. V. Yarmolyuk, I. V. Anisimova, A. M. Sugorakova and Y. V. Plotkina, *Dokl. Earth Sci.*, 2010, **430**, 134–136.
5 Y. H. Yang, F. Y. Wu, H. R. Fan, L. W. Xie and Y. B. Zhang, *Geochim. Cosmochim. Acta*, 2009, **73**, A1481.
6 S. Nakai, A. Masuda and E. Lehmann, *Am. Mineral.*, 1988, **73**, 111–113.
7 F. Y. Wu, Y. H. Yang, L. W. Xie, J. H. Yang and P. Xu, *Chem. Geol.*, 2006, **234**, 105–206.
8 L. W. Xie, Y. B. Zhang, H. H. Zhang, J. F. Sun and F. Y. Wu, *Chin. Sci. Bull.*, 2008, **53**, 1565–1573.
9 D. Günther and C. A. Heinrich, *J. Anal. At. Spectrom.*, 1999, **14**, 1363–1368.
10 K. R. Ludwig, *A geochronological toolkit for microsoft excel. Isoplot*, 2003, vol. 3, pp. 1–70.
11 W. L. Griffin, W. J. Powell, N. J. Pearson and S. Y. O'Reilly, *Mineral. Assoc. Can., Short Course Handb.*, 2008, **40**, 308–311.
12 J. Košler, H. Fonneland, P. Sylvester, M. Tubrett and R. B. Pedersen, *Chem. Geol.*, 2002, **182**, 605–618.
13 D. M. Chew, J. A. Petrus and B. S. Kamber, *Chem. Geol.*, 2014, **363**, 185–199.
14 R. A. Cox and R. H. C. Wilton, *Chem. Geol.*, 2006, **235**, 21–32.
15 J. S. Stacey and J. D. Kramers, *Earth Planet. Sci. Lett.*, 1975, **26**, 207–221.
16 I. S. Williams. U–Th–Pb geochronology by ion microprobe, in *Reviews in Economic Geology*, ed. M. A. McKibben, W. C. Shanks, III III and W. I. Ridley, 1998, vol. 7, pp. 1–35.
17 J. M. Batumike, W. L. Griffin, E. A. Belousova, N. J. Pearson, S. Y. O'Reilly and S. R. Shee, *Earth Planet. Sci. Lett.*, 2008, **267**, 609–619.
18 Y. H. Yang, F. Y. Wu, S. A. Wilde, X. M. Liu, Y. B. Zhang, L. W. Xie and J. H. Yang, *Chem. Geol.*, 2009, **264**, 24–42.
19 S. E. Jackson, N. J. Pearson, W. L. Griffin and E. A. Belousova, *Chem. Geol.*, 2004, **211**, 47–69.
20 J. F. Sun, J. H. Yang, F. Y. Wu, L. W. Xie, Y. H. Yang, Z. C. Liu and X. H. Li, *Chin. Sci. Bull.*, 2012, **57**, 2506–2516.
21 Z. C. Liu, F. Y. Wu, C. L. Guo, Z. F. Zhao, J. H. Yang and J. F. Sun, *Chin. Sci. Bull.*, 2011, **56**, 2948–2956.
22 A. E. Korh, *Spectrochim. Acta, Part B*, 2013, **86**, 75–87.
23 A. E. Korh, *Chem. Geol.*, 2014, **371**, 46–59.
24 C. Xu, I. H. Campbell, J. Kynicky, C. M. Allen, Y. J. Chen, Z. L. Huang and L. Qi, *Lithos*, 2008, **106**, 12–24.
25 Z. Q. Hou, S. H. Tian, Y. L. Xie, Z. S. Yang, Z. X. Yuan, S. P. Yin, L. S. Yi, H. C. Fei, T. R. Zou, G. Bai and X. Y. Li, *Ore Geol. Rev.*, 2009, **36**, 65–89.
26 S. H. Tian, Z. Q. Hou, Z. S. Yang, W. Chen, Z. M. Yang, Z. X. Yuan, Y. L. Xie, H. C. Fei, S. P. Yin, Y. C. Liu, Z. Li and X. Y. Li, *Mineral Deposits*, 2008, **27**, 177–187, (in Chinese with English abstract).
27 S. H. Tian, Z. Q. Hou, Z. S. Yang, Z. M. Yang, Z. X. Yuan, Y. B. Wang, Y. L. Xie, Y. C. Liu and Z. Li, *Acta Petrol. Sin.*, 2008, **24**, 544–554, (in Chinese with English abstract).
28 Z. X. Yuan, Z. M. Shi, G. Bai, C. Y. Wu, R. A. Chi and X. Y. Li, *The Maoniuping Rare Earth Ore Deposit, Mianning County, Sichuan Province,* Seismological Press, Beijing, 1995, p. 150, (in Chinese).
29 G. M. Yang, C. Chang, D. H. Zuo and X. L. Liu, *Geology and Mineralization of the Dalucao REE Deposit in Dechang County, Sichuan Province,* Open file of China University of Geosciences, Wuhan, 1998, pp. 1–89, (in Chinese).